JACS
JOURNAL OF THE AMERICAN CHEMICAL SOCIETY

Article

pubs.acs.org/JACS

A Suite of Tetraphenylethylene-Based Discrete Organoplatinum(II) Metallacycles: Controllable Structure and Stoichiometry, Aggregation-Induced Emission, and Nitroaromatics Sensing

Xuzhou Yan,[*,†] Haoze Wang,[†,‡] Cory E. Hauke,[§] Timothy R. Cook,[§] Ming Wang,[∥] Manik Lal Saha,[†] Zhixuan Zhou,[†] Mingming Zhang,[†] Xiaopeng Li,[∥] Feihe Huang,[*,‡] and Peter J. Stang[*,†]

[†]Department of Chemistry, University of Utah, 315 South 1400 East, Room 2020, Salt Lake City, Utah 84112, United States

[‡]State Key Laboratory of Chemical Engineering, Center for Chemistry of High-Performance & Novel Materials, Department of Chemistry, Zhejiang University, Hangzhou 310027, P. R. China

[§]Department of Chemistry, University at Buffalo, 359 Natural Sciences Complex, Buffalo, New York 14260, United States

[∥]Department of Chemistry and Biochemistry and Materials Science, Engineering, and Commercialization Program, Texas State University, San Marcos, Texas 78666, United States

Supporting Information

ABSTRACT: Materials that organize multiple functionally active sites, especially those with aggregation-induced emission (AIE) properties, are of growing interest due to their widespread applications. Despite promising early architectures, the fabrication and preparation of multiple AIEgens, such as multiple tetraphenylethylene (multi-TPE) units, in a single entity remain a big challenge due to the tedious covalent synthetic procedures often accompanying such preparations. Coordination-driven self-assembly is an alternative synthetic methodology with the potential to deliver multi-TPE architectures with light-emitting characteristics. Herein, we report the preparation of a new family of discrete multi-TPE metallacycles in which two pendant phenyl rings of the TPE units remain unused as a structural element, representing novel AIE-active metal−organic materials based on supramolecular coordination complex platforms. These metallacycles possess relatively high molar absorption coefficients but weak fluorescent emission under dilute conditions because of the ability of the untethered phenyl rings to undergo torsional motion as a non-radiative decay pathway. Upon molecular aggregation, the multi-TPE metallacycles show AIE-activity with markedly enhanced quantum yields. Moreover, on account of their AIE characteristics in the condensed state and ability to interact with electron-deficient substrates, the photophysics of these metallacycles is sensitive to the presence of nitroaromatics, motivating their use as sensors. This work represents a unification of themes including molecular self-assembly, AIE, and fluorescence sensing and establishes structure−property−application relationships of multi-TPE scaffolds. The fundamental knowledge obtained from the current research facilitates progress in the field of metal−organic materials, metal-coordination-induced emission, and fluorescent sensing.

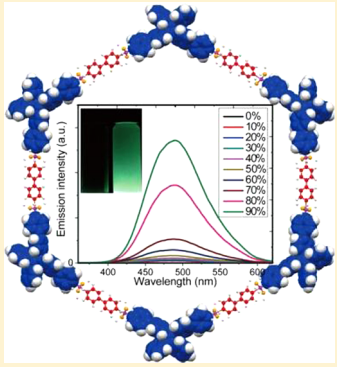

INTRODUCTION

Materials that possess multiple functionalities, such as those with optical, magnetic, and electronic properties, are attractive due to their scientific and technological significance.[1] Light-emitting materials, for example, have attracted considerable attention for their widespread applications in biological and environmental sensors,[2] fluorescent probes,[3] bioimaging agents,[4] light-emitting diodes,[5] and key components of other electronic devices.[6] These applications benefit from the design and exploration of novel fluorescent materials, in particular those with controllable structures and properties.[7] Generally, many chromophores that exhibit highly emissive fluorescence in dilute solutions notoriously suffer from aggregation-caused quenching (ACQ) in concentrated solutions or in the solid state because of the formation of excimers and exciplexes. This influences the practical applications of these fluorophores.[8] Although a variety of physical, chemical, engineering, and supramolecular methods have been developed to address the ACQ effect, it is difficult to circumvent this quenching pathway while maintaining the desirable photophysics of a system.[9] In 2001, an opposite effect known as aggregation-induced emission (AIE) was reported by Tang and co-workers.[10] In such cases, fluorogens that exhibit almost no fluorescence as discrete molecules because of fast non-radiative decay via intramolecular motion in dilute solutions become highly emissive in an aggregated state. The discovery and development of the AIE phenomenon and the realization of various high-tech applications of this effect have seen a rapid advance of research over the past decade.[11] Despite these achievements, the

Received: September 26, 2015
Published: November 9, 2015

DOI: 10.1021/jacs.5b10130
J. Am. Chem. Soc. 2015, 137, 15276−15286

Scheme 1. Self-Assembly of 1 with 2−6 To Give Rhomboid 7 and Hexagons 8−11

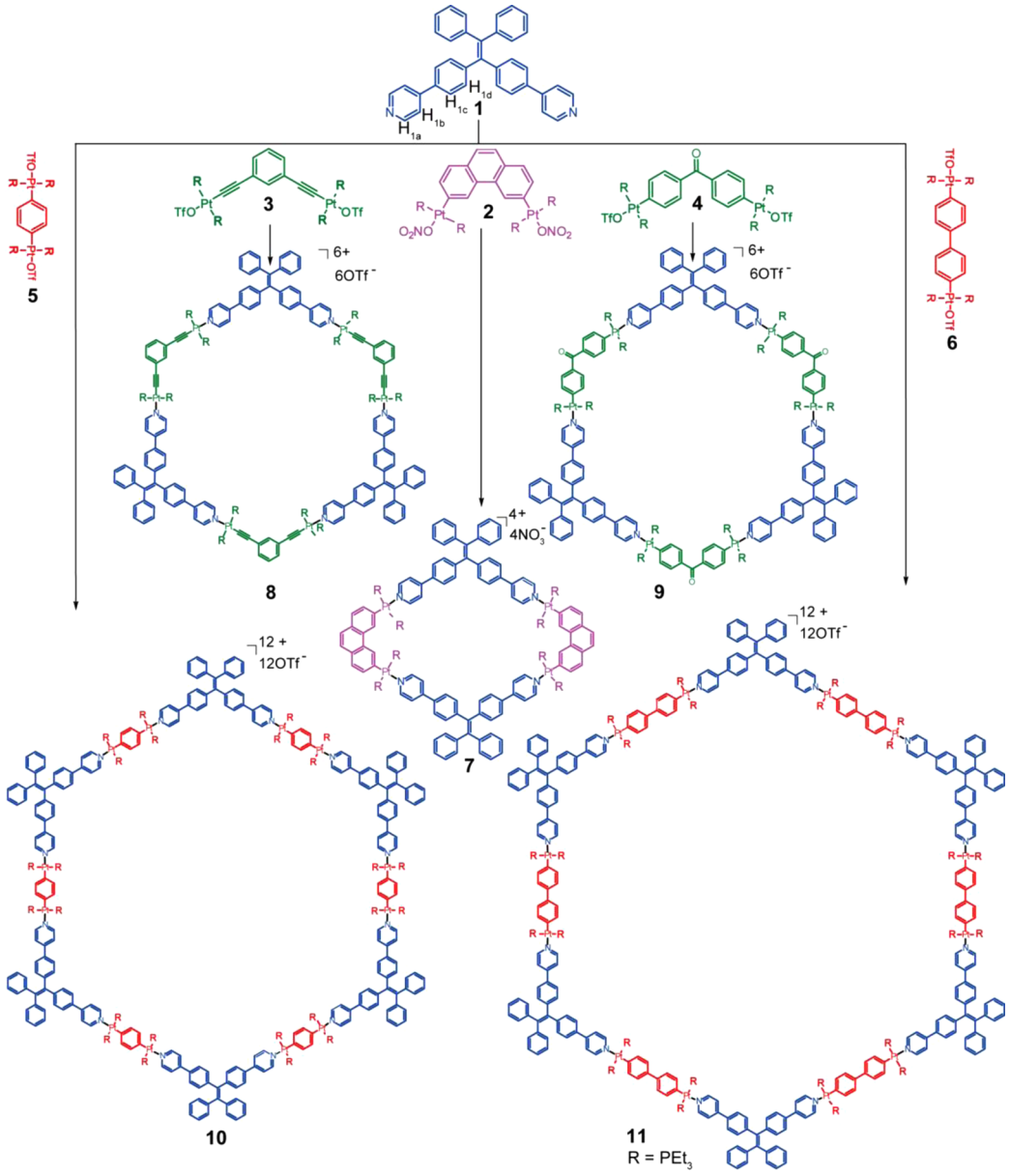

fabrication of AIE-active species primarily draws upon the covalent modification of simple AIEgens;[12] a highly efficient non-covalent self-assembly methodology has rarely been employed to construct architecturally complex and high-order superstructures that take advantage of these emissive features and promising functions.

Coordination-driven self-assembly has been proven to be a powerful tool to construct supramolecular coordination complexes (SCCs) via the spontaneous formation of metal−ligand bonds which have moderate bond energies in the range of 15−25 kcal/mol and predictable coordination geometries. The resultant SCCs are oftentimes stable, despite the reversibility of their coordination chemistry, which helps a given system cascade to a thermodynamic product.[13] Unified under the principle of *directional bonding*, various design and synthetic methodologies underpinning coordination-driven self-assembly have emerged, as developed by Cotton,[14] Stang,[15] Raymond,[16] Mirkin,[17] Fujita,[18] Newkome,[19] Hupp,[20] Schmittel,[21] Shionoya,[22] Nitschke,[23] Jin,[24] and others.[25] This work has produced a sizable library of discrete metallacycles and metallacages with well-defined shapes and sizes. For example, in the Stang laboratory, phosphine-capped Pt(II) nodes and rigid organic donors have been utilized to illustrate how the angularities, directionalities, and stoichiometries of the building blocks dictate an exclusive architectural outcome.[15] In the past two decades, the development and maturation of this research field has witnessed SCCs widely applicable in catalysis,[16,26] molecular flasks,[27] host−guest chemistry,[28] mechanically interlocked structures,[29] template synthesis,[30] amphiphilic self-assembly,[31] supramolecular polymers,[32] and bioengineering.[33] Although quite a few light-emitting metal-coordinated complexes are known,[1d,34] investigations that explore the intriguing photophysical behaviors of phosphine-capped Pt(II) metal−organic complexes toward bioimaging and explosive-sensing applications are rare.

As a well-known and readily accessible AIE fluorogen, tetraphenylethylene (TPE) shows low-frequency phenyl ring rotation and ethylenic C═C bond twist behaviors which can be

DOI: 10.1021/jacs.5b10130
J. Am. Chem. Soc. 2015, 137, 15276−15286

deactivated by tight intermolecular packing in the condensed state to induce fluorescence.[12b] However, the aggregation of TPE chromophores is not the only way to realize turn-on fluorescence: if restriction of intramolecular rotation (RIR) can be achieved by other strategies, a similar phenomenon is observed. For example, several pioneering reports have revealed the anchoring of TPE-based ligands within metal−organic frameworks (MOFs) to afford luminescent materials.[35] Dincă et al. reported the first TPE-based MOF and used the MOF platform to study the low-energy vibrational modes of AIE-type chromophores.[35a,b] Zhou et al. demonstrated that rigidifying the TPE-based linker in a zirconium MOF efficiently adjusts the fluorescence energy and enhances the quantum yield.[35c] Tang, Liu, Zhao, and co-workers constructed a 2D layered TPE-based MOF as a turn-on fluorescent sensor for volatile organic compounds.[35d] Over the past 5 years, a host of noncovalent strategies, including host−guest chemistry,[36] anion-coordination,[37] metal-coordination,[38] hydrogen bonding,[39] $\pi-\pi$ stacking,[40] electrostatic interactions,[41] etc., have been developed to induce AIE-active molecular emission.

Architectures that organize multiple TPE units are attractive in that their strong AIE features make them promising for organic light-emitting diodes and other electronic devices. Despite their value, the preparation of such interesting structures is largely limited to TPE-based MOFs and polymers. This lack of structures is in part attributed to the tedious covalent synthetic procedures that accompany traditional designs.[42] As such, supramolecular self-assembly is a viable strategy due to its reduction in synthetic steps, well-defined organizations of individual components, inherent error-correction and defect-free assembly, and facile and fast formation of final products.[43] Stimulated by these advantages, we envisioned that the preparation of discrete multiple TPE-based architectures on SCC platforms could be achieved by combining a TPE-based dipyridyl ligand and appropriately designed organoplatinum(II) acceptors via metal-coordination-driven self-assembly. This methodology makes for the resulting discrete assemblies with controllable shape and size along with precise distribution and total number of anchored TPE moieties. Moreover, fine-tuning the shape, size, distribution, and distance between different TPE motifs enables an understanding of the influence of structural factors on the light-emitting behaviors of the architectures.

Recently, our group reported the first TPE-based highly emissive discrete SCC, formed by locking two TPE-based ligands within a tetragonal prismatic core wherein non-radiative decay pathways were eliminated. This system was used to efficiently differentiate structurally similar ester compounds.[44] Whereas the TPE rings were locked in this earlier design, we anticipated that a TPE-based ligand bearing two freely rotating phenyl rings might be useful for the formation of responsive fluorescent sensing materials due to a decrease in the activation barrier for ring-flipping in the TPE moieties. In this work, we report the design and construction of a new family of multi-TPE discrete organoplatinum(II) metallacycles via coordination-driven self-assembly, in which two dangling phenyl rings in the TPE units remain unrestricted, representing a novel AIE-active metal−organic material based on SCC platforms. When the 120° TPE-based dipyridyl ligand was combined with suitable 60°, 120°, and 180° organoplatinum(II) acceptors, a suite of metallacycles was obtained. These metallacycles were formed in nearly quantitative yields by means of the *directional-bonding approach* driven by metal-coordination. Each species exhibited relatively high molar absorption coefficients but weak fluorescent emission because of the existence of freely rotating phenyl rings. Upon molecular aggregation, the fluorescent intensities underwent obvious enhancements along with increased quantum yields. Inspired by their emissive characteristics in the condensed state, we further utilized multi-TPE metallacycles **7**, **8**, and **11** to detect picric acid with quenching constant and detection limit reaching up to $2.18 \times 10^6\ M^{-1}$ and 0.13 ppb, respectively. The methodology developed here represents a promising way to construct light-emitting metal−organic materials with intriguing sensing applications based on SCC platforms.

RESULTS AND DISCUSSION

According to the principle of *directional bonding*, the directionality and angularity of each component involved in the coordination-driven self-assembly dictate the final architectural outcome, wherein the discrete SCCs with well-defined shape and size can be easily prepared with high efficiency.[15] In this study, a 120° TPE-based dipyridyl ligand, **1**, and di-Pt(II) acceptors, **2**−**6**, were combined to furnish rhomboid **7** and different sized hexagons **8**−**11** (Scheme 1), respectively.

Ligand **1** was readily synthesized by a Pd-catalyzed Suzuki coupling (Scheme S1). Stirring a mixture of **1** with 60° di-Pt(II) acceptor **2**, 120° di-Pt(II) acceptor **3** or **4**, or 180° di-Pt(II) acceptor **5** or **6** in a 1:1 ratio in CD_2Cl_2 at room temperature for 8 h, led to the formation of the self-assembled [2+2] rhomboid **7**, the [3+3] hexagon **8** or **9**, and the [6+6] hexagon **10** or **11**, respectively (Scheme 1).

Multinuclear NMR (^1H and ^{31}P) analysis of the reaction mixture supported the formation of discrete multi-TPE metallacycles with highly symmetric constructs. The $^{31}P\{^1H\}$ NMR spectra of **7**−**11** exhibited sharp singlets (ca. 14.05 ppm for **7**, 16.81 ppm for **8**, 14.11 ppm for **9**, 13.99 ppm for **10**, and 14.72 ppm for **11**) with concomitant ^{195}Pt satellites corresponding to a single phosphorus environment (Figure 1). These peaks are shifted upfield from those of the corresponding starting di-Pt(II) acceptors **2**, **3**, **4**, **5**, and **6** by approximately 4.54, 5.20, 4.14, 5.04, and 5.04 ppm, respectively. This change as well as the decrease in coupling of the flanking ^{195}Pt satellites (ca. $\Delta J = -188.2$ Hz for **7**, $\Delta J = -30.40$ Hz for

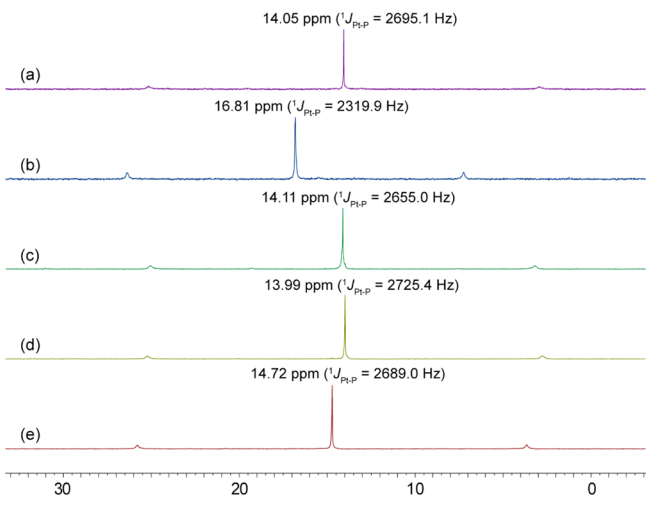

Figure 1. $^{31}P\{^1H\}$ NMR spectra (121.4 M, CD_2Cl_2, 293 K) of rhomboid **7** (a), [3+3] hexagon **8** (b), [3+3] hexagon **9** (c), [6+6] hexagon **10** (d), and [6+6] hexagon **11** (e).

DOI: 10.1021/jacs.5b10130
J. Am. Chem. Soc. 2015, 137, 15276−15286

8, ΔJ = −191.8 Hz for **9**, ΔJ = −152.9 Hz for **10**, and ΔJ = −144.5 Hz for **11**) is consistent with the electron back-donation from the platinum centers. In the ^{1}H NMR spectrum of rhomboid **7** (Figure 2, spectrum b), signals corresponding to the H_{1a-d} protons of the pyridine and phenyl rings displayed downfield shifts relative to those of the free TPE ligand **1** because of the loss of electron density that occurs upon the Pt−N bond formation. As shown in Figure 2 (spectrum b), the H_{1a} and H_{1b} protons on the pyridine rings are split into two sets of two doublets upon metal-coordination, which is consistent with the previously reported 120° 1,3-bis(4-pyridylethynyl)benzene derivative ligand-based organoplatinum(II) rhomboids.[34c] The H_{1a} protons which appear as a doublet at 8.62 ppm in the spectrum of **1** (Figure 2, spectrum a) are split into two doublets at 9.07 and 8.71 ppm for **7** (Figure 2, spectrum b). Similarly, the H_{1b} protons (7.50 ppm in **1**; Figure 2, spectrum a) are also split into two doublets, at 8.04 and 7.83 ppm (Figure 2, spectrum b). As for hexagonal multi-TPE metallacycles, downfield shifts of the H_{1a-d} protons of the pyridine and phenyl rings relative to those of **1** were also observed (Figure 2, spectra c−f). In the ^{1}H NMR spectrum of hexagon **9** (Figure 2, spectrum d), for example, sharp signals corresponding to coordinated H_{1a-d} pyridyl and phenyl protons were assigned at 8.72, 7.98, 7.72, and 7.31 ppm with downfield shifts relative to those of **1** (ca. $\Delta\delta$ = 0.10 ppm for H_{1a}, $\Delta\delta$ = 0.48 ppm for H_{1b}, $\Delta\delta$ = 0.25 ppm for H_{1c}, and $\Delta\delta$ = 0.10 ppm for H_{1d}). The well-defined signals in both the ^{31}P{^{1}H} and ^{1}H NMR spectra as well as the good solubility of these species support the formation of a discrete structure as a sole assembly product.

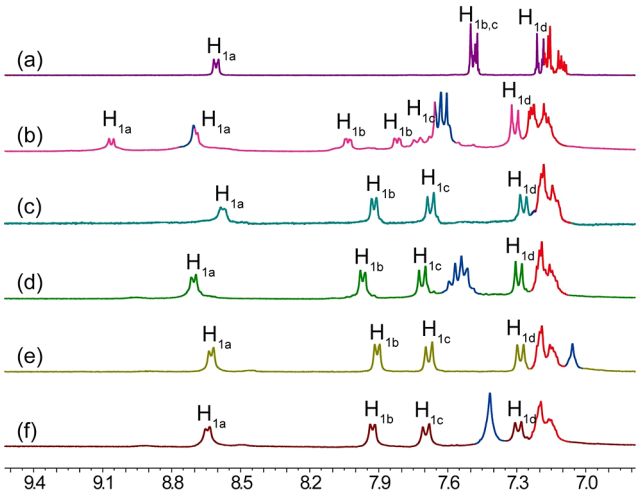

Figure 2. Partial ^{1}H NMR spectra (300 M, CD_2Cl_2, 293 K) of TPE-based ligand **1** (a), [2+2] rhomboid **7** (b), [3+3] hexagon **8** (c), [3+3] hexagon **9** (d), [6+6] hexagon **10** (e), and [6+6] hexagon **11** (f). The peaks for protons of the TPE units are red and those of the acceptors are blue.

Electrospray ionization time-of-flight mass spectrometry (ESI-TOF-MS) is a highly reliable tool to provide evidence for the stoichiometry of formation of multi-charged supramolecular structures. This method oftentimes enables metallacycles to remain intact during the ionization process while producing the high resolution desired for isotopic distribution analysis.[25g,h] The ESI-TOF-MS characterizations gave further evidence for the existence of multi-TPE metallacycles **7**−**11**. In the ESI-TOF-MS spectrum of **7**, three peaks were assigned that agree with the formation of a [2+2] assembly (Figure S17). These peaks corresponded to an intact entity with charge states arising from the loss of counterions [m/z = 1586.51 for $[M - 2NO_3]^{2+}$, m/z = 1037.70 for $[M - 3NO_3]^{3+}$ (Figure 3a), and m/z = 762.24 for $[M - 4NO_3]^{4+}$]. For **8** and **9**, four peaks were identified for each assembly to support the formation of a [3+3] assembly (Figures S21 and S25), e.g., m/z = 1179.64, corresponding to $[M - 4OTf]^{4+}$ for **8** (Figure 3b), and m/z = 947.51 corresponding to $[M - 5OTf]^{5+}$ for **9** (Figure 3c). Similarly, three peaks were found for **10** and **11** to support the formation of a [6+6] assembly (Figures S29 and S33), e.g., m/z = 1918.67, corresponding to $[M - 5OTf]^{5+}$ for **10** (Figure 3d) and m/z = 1393.31, corresponding to $[M - 7OTf]^{7+}$ for **11** (Figure 3e). All the assigned peaks were isotopically resolved and in good agreement with their calculated theoretical distributions, which indicated the molecularity of these multi-TPE metallacycles.

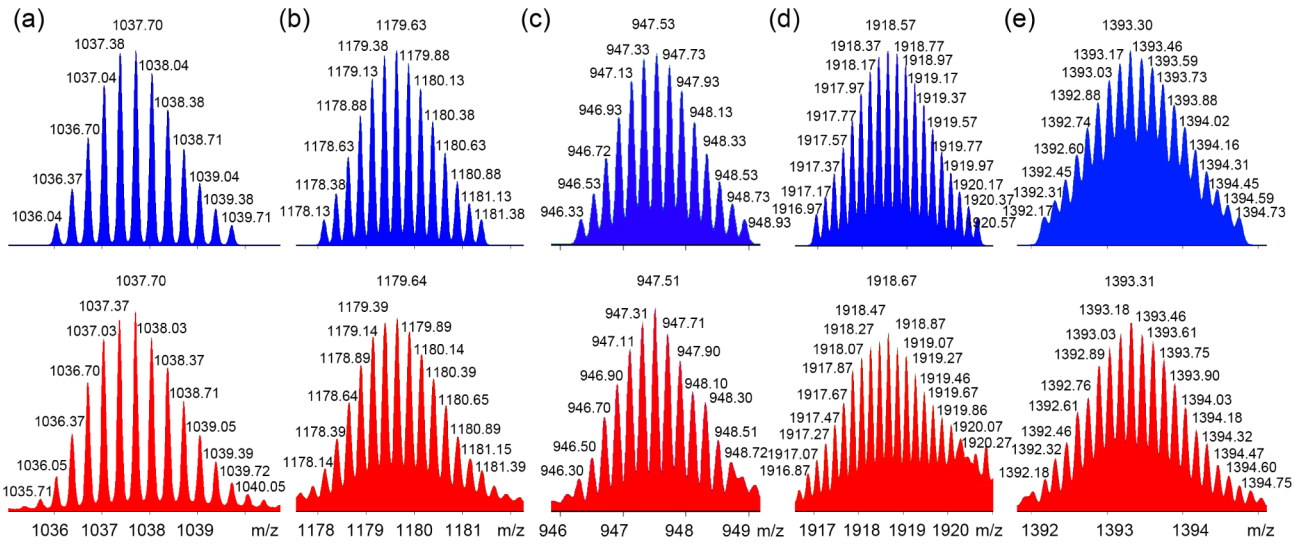

Figure 3. Experimental (red) and calculated (blue) ESI-TOF-MS spectra of multi-TPE metallacycles: (a) **7** $[M - 3NO_3]^{3+}$, (b) **8** $[M - 4OTf]^{4+}$, (c) **9** $[M - 5OTf]^{5+}$, (d) **10** $[M - 5OTf]^{5+}$, and (e) **11** $[M - 7OTf]^{7+}$.

DOI: 10.1021/jacs.5b10130
J. Am. Chem. Soc. 2015, 137, 15276−15286

In view of the difficulty associated with growing single crystals of these assemblies suitable for X-ray diffraction, molecular simulations were performed to obtain further insight into the architectural features of multi-TPE metallacycles **7**−**11** (Figure 4). All DFT calculations were performed using

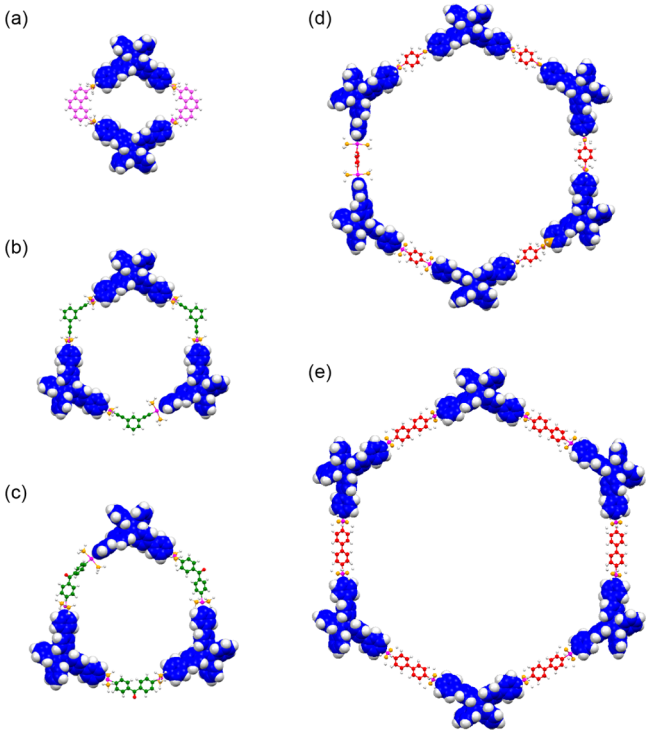

Figure 4. Simulated molecular models of multi-TPE metallacycles **7** (a), **8** (b), **9** (c), **10** (d), and **11** (e). The metallacycles **7**−**9** were optimized via density functional theory, and PM6 semiempirical molecular orbital method was used for **10** and **11**.

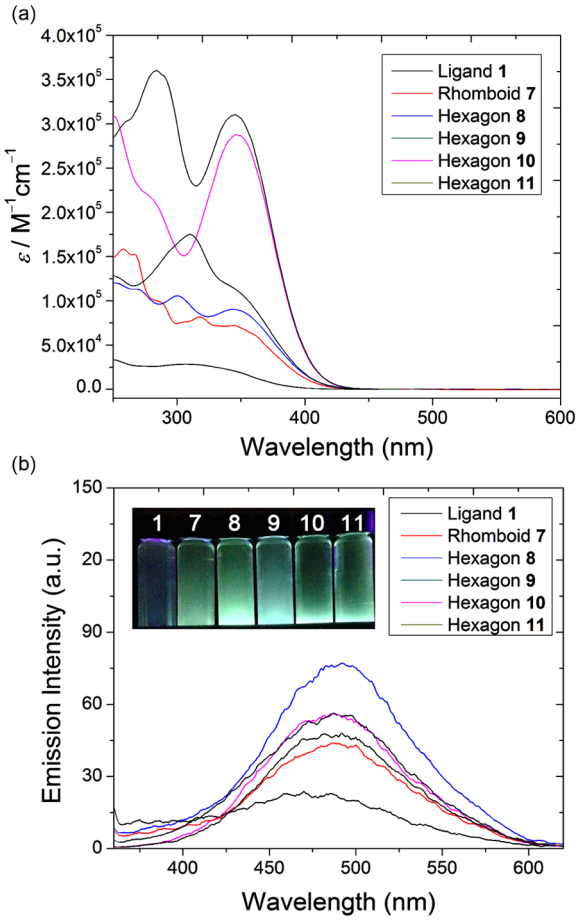

Figure 5. (a) Absorption and (b) fluorescence emission spectra of ligand **1** and multi-TPE metallacycles **7**−**11** in CH_2Cl_2 (λ_{ex} = 320 nm, c = 10.0 μM). Inset: photograph of **1** and **7**−**11** in CH_2Cl_2 upon excitation at 365 nm using an UV lamp at 298 K (c = 10.0 μM).

Gaussian09 (G09)[45] with the Becke three-parameter hybrid exchange and the Lee−Yang−Parr correlation functional (B3LYP).[46] The 6-31G** basis set[47] was used for H, C, N, O and P atoms, while the Los Alamos National Laboratories (LANL2DZ) basis set[48] and pseudopotential was used for Pt. All geometry optimizations were performed without a solvent field in C1 symmetry; the results are in the gas phase. To minimize computational cost, the PEt_3 ligands on platinum were modeled as PH_3 ligands. The PM6 calculations were also carried out with Gaussian 09. The simulated structure of bis-TPE rhombiod **7** possesses a well-defined rhombus with a ca. 2.4 × 2.0 nm cavity (Figure 4a). Similarly, molecular simulations showed very similar, roughly planar hexagonal structures for hexagons **8**−**11**, albeit with differing cavity sizes (3.2 × 2.9 nm for **8**, 3.4 × 3.0 nm for **9**, 5.6 × 5.0 nm for **10**, and 6.5 × 5.8 nm for **11**) (Figure 4b−e). The simulated structures revealed that the coordination vectors as defined by the N−Pt axes adopt a ca. 118° angle with a ca. 114° angle between the two dangling phenyl rings, which is responsible for the weakly emissive fluorescence of these multi-TPE metallacycles (*vide infra*). In addition, all of the dangling phenyl rings are aligned along the outer vertexes of these metallacycles, poising these groups for participating in AIE (*vide infra*).

The absorption spectra of ligand **1** and multi-TPE metallacycles **7**−**11** are shown in Figure 5a. Ligand **1** displayed a broad absorption band centered at 310 nm with a molar absoprtion coefficient (ε) of 2.83 × 10^4 M^{-1} cm^{-1}. After metal-coordination, the lowest energy band moderately red-shifted (~36 nm) in the spectra of the corresponding metallacycles. In the absorption profile of **7**, there are four absorption bands at 257, 285, 317, and 345 nm with ε = 1.59 × 10^5, 9.99 × 10^4, 8.18 × 10^4, and 7.13 × 10^4 M^{-1} cm^{-1}, respectively. There are two absorption bands centered at 300 and 346 nm for **8**, 310 and 347 nm for **9**, 283 and 347 nm for **10**, and 284 and 345 nm for **11**.

Figure 5b displays the fluorescence emission spectra of **1** and metallacycles **7**−**11**. Ligand **1** is weakly emissive at ca. 470 nm in CH_2Cl_2. This lack of emission is attributed to non-radiative decay via intramolecular rotations of the pyridyl and phenyl rings. Partially rigidifying the weakly emissive TPE ligand into rigid, discrete metallacycles induced some fluorescence enhancements and the emission maximum of **1** underwent a moderate red shift from 470 to 490 nm in CH_2Cl_2 at room temperature. According to the TPE-based AIE mechanism, a given emission wavelength shift is usually correlated with a specific conformation of the peripheral phenyl rings: a coplanar conformation promotes π-electron conjugation resulting in a red shift and a perpendicular conformation weakens π-electron conjugation, thus leading to a blue shift.[49] In addition to rigidification from metallacycle-formation, new metal-to-ligand charge-transfer (MLCT) processes are enabled upon coordination. These effects manifest in a shift from blue to cyan

DOI: 10.1021/jacs.5b10130
J. Am. Chem. Soc. 2015, 137, 15276−15286

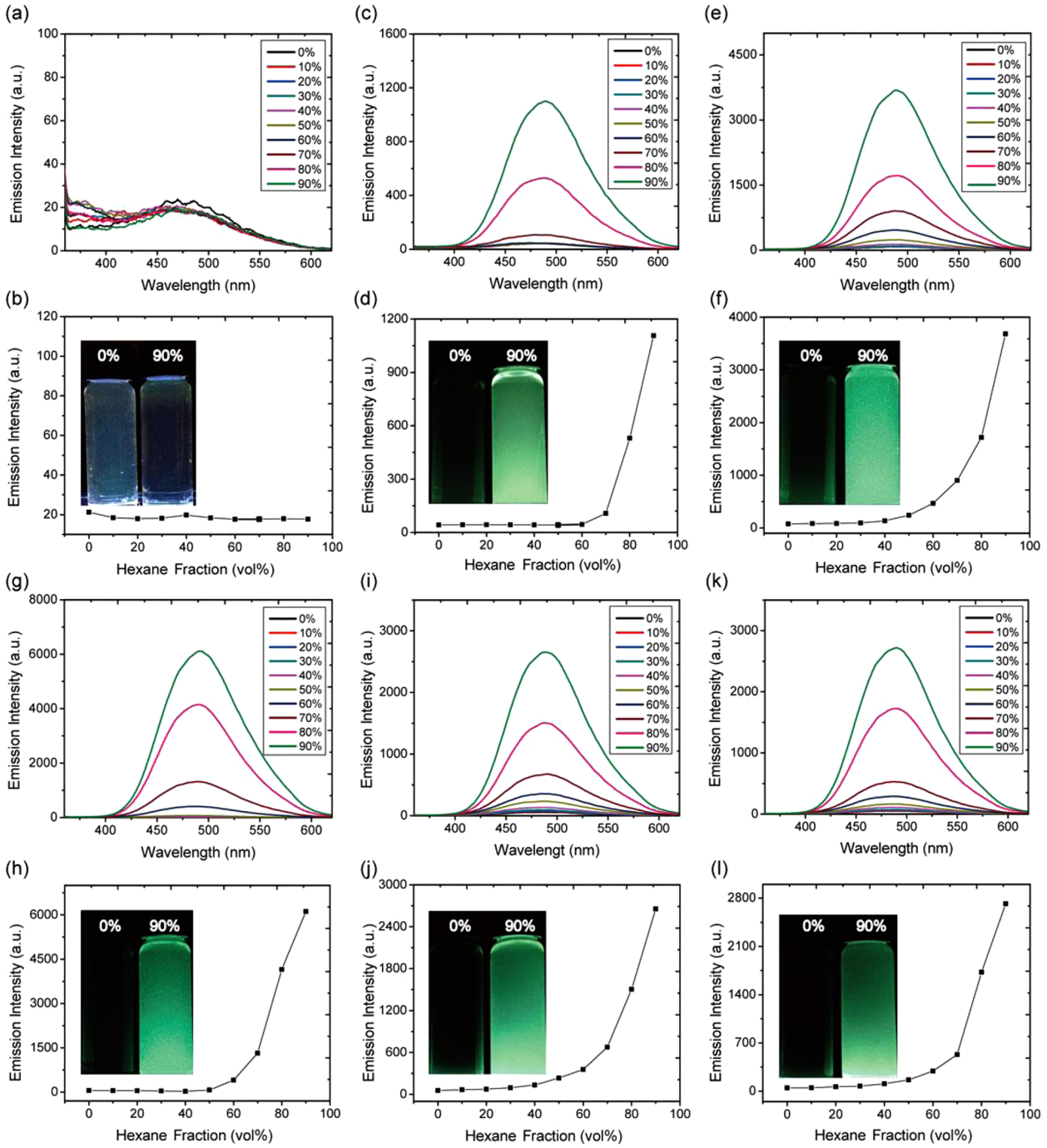

Figure 6. Fluorescence emission spectra and plots of maximum emission intensity of ligand **1** (a,b), **7** (c,d), **8** (e,f), **9** (g,h), **10** (i,j), and **11** (k,l) versus hexane fraction in CH_2Cl_2/hexane mixtures (λ_{ex} = 320 nm, c = 10.0 μM). Insets: photographs of **1** and **7**−**11** in CH_2Cl_2 and 10%/90% CH_2Cl_2/hexane mixture upon excitation at 365 nm using an UV lamp at 298 K (c = 10.0 μM).

emission after metal-coordination (see the inset of Figure 5b). In these multi-TPE metallacycles, the limited fluorescence enhancement suggests that the TPE units are not sufficiently rigidified to remove non-radiative decay pathways.

In order to investigate the AIE properties of **1** and **7**−**11**, the fluorescence emission in CH_2Cl_2 and CH_2Cl_2/hexane mixture solutions were recorded (Figure 6). The emission intensity and peak wavelength of **1** showed no obvious change in CH_2Cl_2/hexane solutions because of the solubility (Figure 6a,b), indicating that it is not an AIE-active chromophore in such mixed solvent systems. Dilute CH_2Cl_2 solutions of **7** displayed very weak fluorescence and the emission intensity remained low in mixed solutions with hexane content less than 70%. However, upon further increasing the hexane content to 90%, the fluorescence intensity (λ_{max} = 490 nm) increased greatly (Figure 6c,d). Moreover, the absorption spectra of **7** in the CH_2Cl_2/hexane solutions were also recorded. The appearance of broad tails into the visible region supported the formation of aggregates (Figure S34b). These collective results suggested that rhomboid **7** was AIE-active. The AIE phenomenon observed in **7** is not an isolated case, is also found in hexagons **8**−**11** (Figures 6e−l and S29c−f). For example, upon

DOI: 10.1021/jacs.5b10130
J. Am. Chem. Soc. 2015, 137, 15276−15286

increasing the hexane fraction to 90%, the emission intensities of **8**–**11** clearly increased (Figures 6e–l). Moreover, an increase in the total number of TPEs in the metallacyclic frameworks resulted in reduced solubilities and ultimately meant that aggregation occurred at lower hexane percentages (Figures 6 and S35). The pendant phenyl rings which provided non-radiative relaxation pathways presumably rigidify upon aggregation, resulting in the marked emission enhancements observed.

The changes in quantum yields (Φ_F) of **7**–**11** in mixed solvent solutions further demonstrated the AIE characteristics of these assemblies (Figure 7). In CH_2Cl_2, relatively low Φ_F values were determined: 0.088% for **7**, 0.25% for **8**, 0.19% for **9**, 0.15% for **10**, and 0.14% for **11**. The Φ_F value of **7** remained almost unchanged until 80% hexane. Tris-TPE hexagons **8** and **9** and hexa-TPE hexagons **10** and **11** started to aggregate at a 50% hexane fraction, as indicated by a rise in their Φ_F values (Figure 7). At a 90% hexane content, the Φ_F values of **7**–**11** reached 1.83%, 6.90%, 10.2%, 3.19% and 2.82%, respectively. The solid-state quantum yields of all five metallacycles were measured by collecting the precipitated assemblies and recording their emission within an integrating light sphere. In all cases, the solid-state Φ_F values followed the same trend observed in Figure 7. The values of 4.6 ± 1.2% (**7**), 19.8 ± 1.0% (**8**), 35.2 ± 0.80% (**9**), 7.0 ± 0.34% (**10**), and 9.6 ± 1.3% (**11**) are all higher than those determined for the 90% hexane solutions, consistent with an AIE mechanism. It is noteworthy that the tris-TPE hexagons **8** and **9** display higher Φ_F values than those of hexa-TPE hexagons **10** and **11** both in solution and in the aggregated state. There is literature precedent that the presence of Pt-ethynyl motifs imparts emissive behavior to a molecule,[50c] and thus **8** has the highest Φ_F value in CH_2Cl_2. In the aggregated state, because hexa-TPE hexagons **10** and **11** have larger metallacyclic skeletons which may restrict the tight packing of TPE units, they showed relatively poorer fluorescent performance than that of **8** and **9** since movement of the phenyl rings is not well restricted. The quantum yield trend suggests that structural factors, such as shape, size, distribution, distance between AIE-active ligands, etc. have an important influence on the light-emitting properties of multi-TPE metal–organic materials.

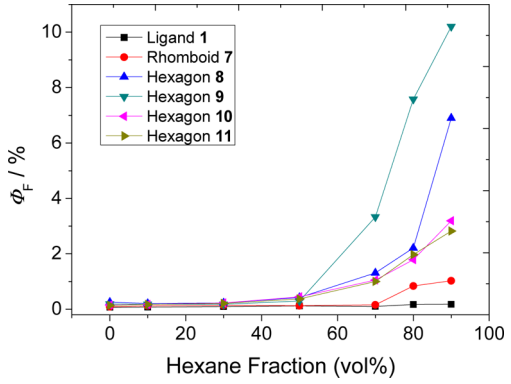

Figure 7. Quantum yields of **1** and **7**–**11** versus hexane fraction in CH_2Cl_2/hexane mixtures which were determined using quinine sulfate at 365 nm (Φ_F = 56%).

The wide use of explosives in industrial manufacturing and military operations not only contaminates the environment but also poses a threat to human health.[50] Inspired by the promising light-emission characteristics of multi-TPE metallacycles in the condensed state, we explored these metallacycles

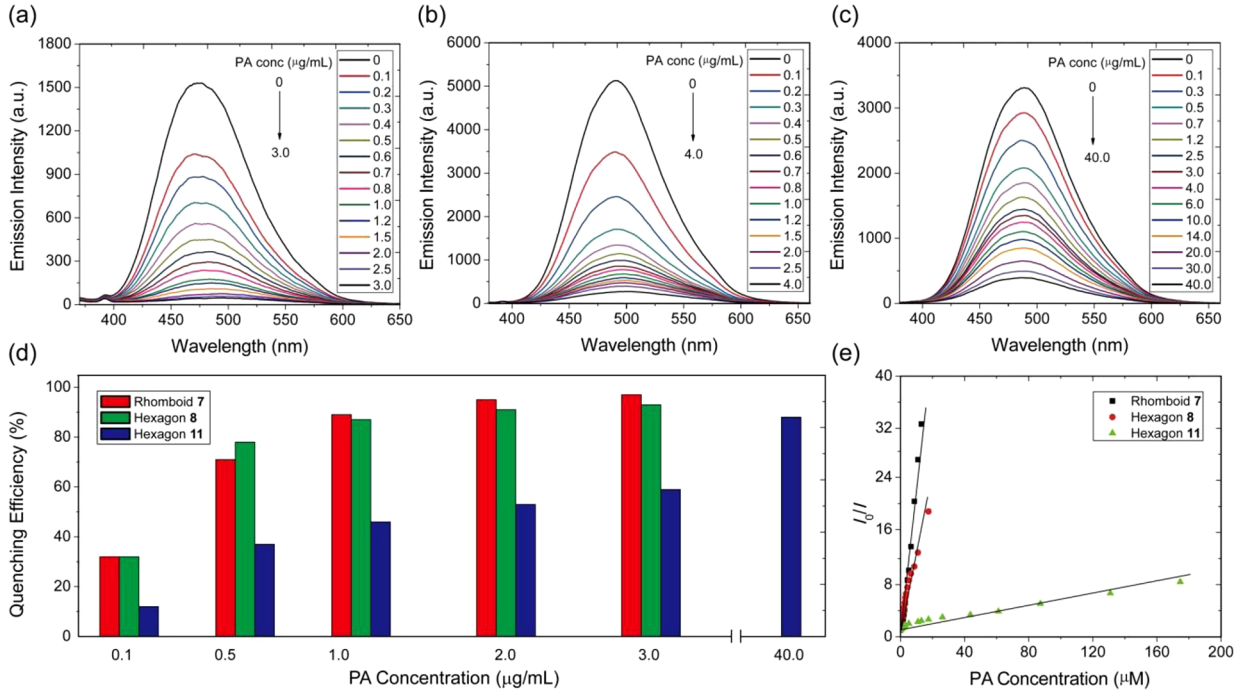

Figure 8. Fluorescence emission spectra of bis-TPE rhomboid **7** (a), tris-TPE hexagon **8** (b), and hexa-TPE hexagon **11** (c) in 10%/90% CH_2Cl_2/hexane mixture containing different amounts of picric acid (PA) (λ_{ex} = 350 nm, c = 10.0 μM). (d) The fluorescence quenching efficiencies of **7**, **8**, and **11** at different picric acid concentrations in 10%/90% CH_2Cl_2/hexane mixture. (e) Plot of relative fluorescence intensities (I_0/I, I = peak intensity and I_0 = peak intensity at [PA] = 0 μM) versus picric acid concentrations in 10%/90% CH_2Cl_2/hexane mixture (λ_{ex} = 350 nm, c = 10.0 μM).

DOI: 10.1021/jacs.5b10130
J. Am. Chem. Soc. 2015, 137, 15276–15286

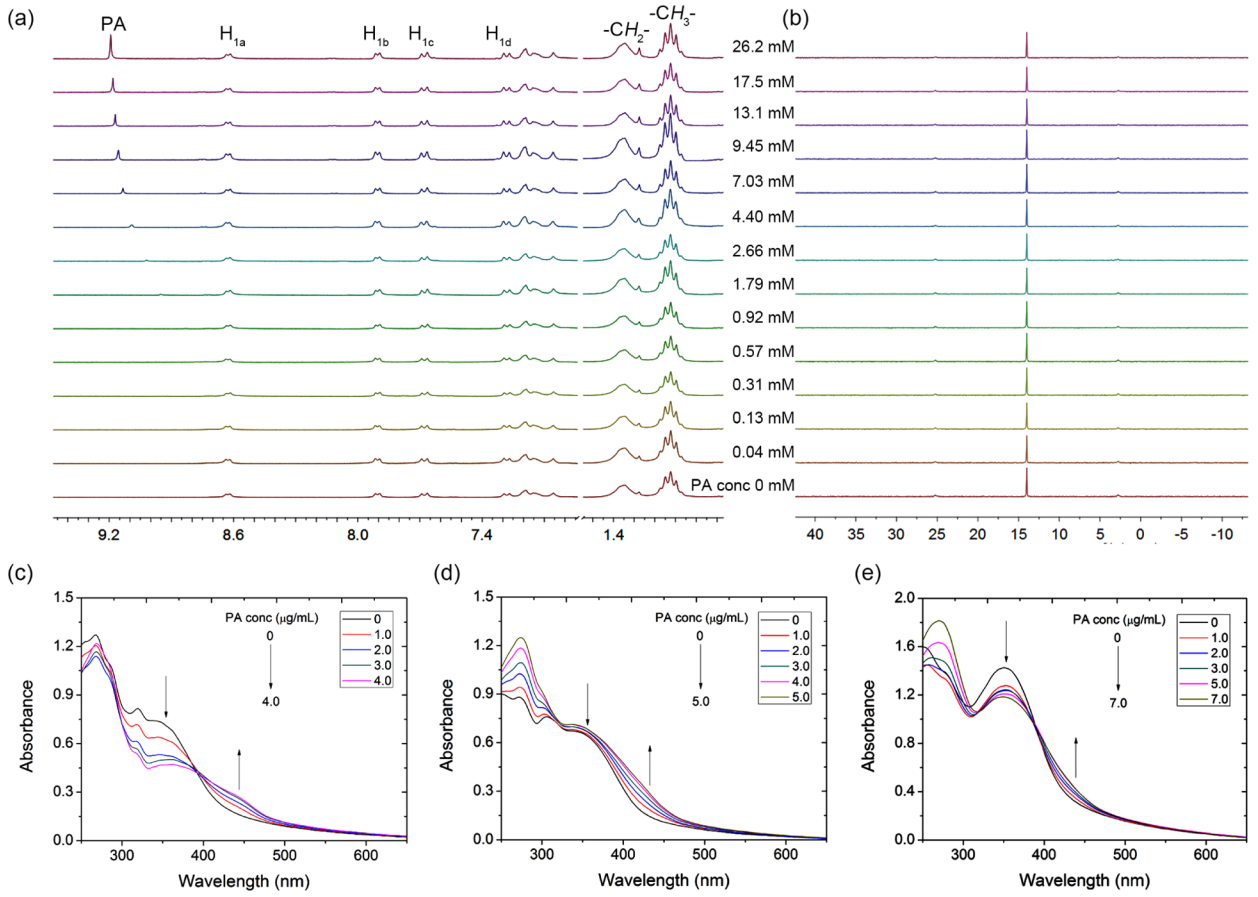

Figure 9. Partial (a) ^{1}H and (b) $^{31}P\{^{1}H\}$ NMR spectra (CD_2Cl_2, 293 K) of hexagon **10** at a concentration of 1.00 mM upon the addition of PA from 0 to 26.2 mM. Absorption spectra (c = 10.0 μM) of **7** (c), **8** (d), and **11** (e) in 10%/90% CH_2Cl_2/hexane mixture containing different amounts of PA.

as chemosensors for the detection of explosive molecules. Nitroaromatics such as 2,4-dinitrotoluene (DNT), 2,4,6-trinitrotoluene (TNT), and 2,4,6-trinitrophenol (TNP; picric acid, PA) are exemplary explosive molecules. We first utilized PA as a model explosive to test the potential sensing abilities of these multi-TPE metallacycles. The aggregates of bis-TPE rhomboid **7**, tris-TPE hexagon **8**, and hexa-TPE hexagon **11** in the CH_2Cl_2/hexane mixture with 90% hexane content were selected as turn-off fluorescent probes for the explosives detection. The quenching processes were monitored by emission intensity changes in response to PA addition (Figure 8a–c). For example, Figure 8a shows that the emission of **7** was attenuated with an increasing amount of PA in the mixed solution. The fluorescence quenching can be clearly observed at a PA concentration as low as 0.1 μg/mL or 0.1 ppm, which is comparable to TPE-based polymers.[51] When the PA concentration was increased to 3.0 μg/mL, there were almost no fluorescence signals. In contrast, other nitro analytes, such as nitrobenzene (NB), 4-nitrotoluene (4-NT), 1,3-dinitrobenzene (1,3-DNB), and 2,4-dinitrotoluene (2,4-DNT), had minor effects on the fluorescence intensity of **7** in the mixed solution (Figure S36), establishing a high selectivity of **7** toward PA over others. Moreover, the detection of PA in aqueous media is feasible by preparing the aggregate of **7** in the acetone/H_2O mixture with 90% H_2O content (Figure S38).

Although hexagon **8** also showed high sensitivity (Figure 8b), hexagon **11** did not show the same degree of quenching efficiency (Figure 8c). As shown in Figure 8d, nearly 32% of fluorescence quenching occurred when 0.1 μg/mL of PA was added to the mixed solutions of **7** and **8**. Under the same condition, just 12% of fluorescence quenching was observed for **11**. At a 3.0 μg/mL PA concentration, the initial fluorescence intensities of **7** and **8** were reduced by 97% and 93%, respectively, but only 59% for **11**. Even at 40.0 μg/mL, only 88% fluorescence quenching was reached for **11** (Figure 8d). With the aim to measure the quenching constants of **7**, **8**, and **11** with PA, the relative fluorescence intensity (I_0/I) was plotted against the PA concentration, which resulted in a linear slope (Figure 8e). Therefore, we employed a linear Stern–Volmer equation $I_0/I = K[PA] + 1$.[52] From the linear fitting, the quenching constants of multi-TPE metallacycles were calculated to be 2.18×10^6 M^{-1} for **7**, 1.13×10^6 M^{-1} for **8**, and 4.50×10^4 M^{-1} for **11**, which are among the high values reported for metal–organic materials.[50b,c,53] The detection limits were determined to be 0.13 ppb for **7**, 9.20 ppb for **8**, and 48.0 ppb for **11** (S/N = 3). The large difference in quenching constants of **7**, **8**, and **11** originated from their structural differences. The hexa-TPE hexagon **11** has the largest metallacyclic skeleton which may restrain the tight packing of TPE units in the aggregated state to some extent, further affecting its fluorescence quenching with PA.

The nature of quenching was further explored using ^{1}H and ^{31}P NMR titration experiments with solutions of a constant concentration of **10** (1.00 mM) and varying concentrations of PA (0–26.2 mM) (Figure 9a,b). In addition, the interaction of PA with ligand **1** was explored. Although the pyridyl groups of

DOI: 10.1021/jacs.5b10130
J. Am. Chem. Soc. 2015, 137, 15276–15286

ligand **1** can interact with PA resulting in downfield shifts of signals for H_{1a-d} on **1** and upfield shifts of the peaks for the aromatic protons of PA (Figure S39), the metallacycle is still intact in the presence of PA. As shown in Figure 9a, with an increasing amount of PA, there are no obvious chemical shift changes of the signals for protons H_{1a-d} on the ligand and for the ethyl protons on the organoplatinum(II) acceptor, indicating that metallacyclic assembly is stable in the presence of PA. ^{31}P NMR spectra also support the stability of Pt−N coordination bonds in the presence of high concentrations of PA (Figure 9b). However, it is worth noting that the aromatic signals of PA underwent downfield shifts upon increased concentration, an opposite shift to the interaction between **1** and PA (Figure S39). This implies the occurrence of non-destructive interactions between metallacycle and PA. Since the absorption spectrum of PA and the emission spectra of the metallacycles has no spectral overlap (Figure S40), FRET mechanisms can be excluded as the origin of quenching. However, the absorption spectra of metallacycles **7**, **8**, and **11** showed a decreased intensity of their lowest energy bands with the appearance of new bands at ca. 440 nm with the addition of PA (Figure 9c−e). The NMR and UV−vis experiments indicate the presence of steady-state interactions that are consistent with a static quenching mechanism due to the formation of non-emissive ground-state complexes.[53]

CONCLUSION

In summary, we have synthesized and characterized a new suite of multi-TPE metallacycles. These species were evaluated for their ability to act as chemosensors for nitroaromatic molecules because of their AIE characteristics. Specifically, a novel 120° TPE-based dipyridyl ligand was designed and synthesized, from which multi-TPE metallacycles were constructed by means of the *directional-bonding approach* through metal-coordination-driven self-assembly. The strategy used here allows for precise control over the metallacyclic size and shape along with the distribution and total number of anchored TPE moieties. The syntheses are straightforward, with almost quantitative yields and without the need of purification. All of the multi-TPE metallacycles were fully characterized by multinuclear NMR (^1H and ^{31}P) and ESI-TOF-MS. The versatility, high efficiency, and modularity of metal-coordination-driven self-assembly were maintained in this system, demonstrating this approach as a strategy to obtain multi-TPE architectures.

These metallacycles exhibited increased molar absorption coefficients from 2.83×10^4 to 3.11×10^5 M^{-1} cm^{-1} after metal-coordination, but relatively weak fluorescent emission because of the existence of freely rotating phenyl rings. Upon molecular aggregation, the multi-TPE metallacycles clearly displayed AIE-activity, which was reflected by fluorescence enhancements as well as increased quantum yields. On account of their AIE characteristics in the condensed state, multi-TPE metallacycles **7**, **8**, and **11** were further explored to detect a model explosive, picric acid, which showed high quenching constants so as to be listed among the high values reported for metal−organic materials, thus making them highly sensitive chemosensors for explosives. These findings provide a comprehensive understanding of the influence of structural factors on the light-emitting properties and sensing applications of multi-TPE metallacycles, which pave a promising route to access elaborate metal−organic materials based on SCC platforms by coordination-driven self-assembly. Efforts to clarify the influence of metal-coordination on light-emitting efficiency of SCCs and the construction of advanced multi-TPE SCCs with unprecedented host−guest and optoelectronic properties are ongoing.

ASSOCIATED CONTENT

Supporting Information

The Supporting Information is available free of charge on the ACS Publications website at DOI: 10.1021/jacs.5b10130.

Experimental details and additional data (PDF)

AUTHOR INFORMATION

Corresponding Authors

*x.yan@utah.edu

*fhuang@zju.edu.cn

*stang@chem.utah.edu

Notes

The authors declare no competing financial interest.

ACKNOWLEDGMENTS

P.J.S. thanks the NSF (Grant 1212799) for financial support. F.H. thanks the National Basic Research Program (2013CB834502), the NSFC/China (21125417), and the State Key Laboratory of Chemical Engineering for financial support. X.L. thanks the NSF (CHE-1506722) and PREM Center of Texas State University (DMR-1205670) for financial support.

REFERENCES

(1) (a) Yan, X.; Wang, F.; Zheng, B.; Huang, F. *Chem. Soc. Rev.* **2012**, *41*, 6042. (b) Colson, J. W.; Dichtel, W. R. *Nat. Chem.* **2013**, *5*, 453. (c) Lehn, J.-M. *Angew. Chem., Int. Ed.* **2015**, *54*, 3276. (d) Yam, V. W.-W.; Au, V. K.-M.; Leung, S. Y.-L. *Chem. Rev.* **2015**, *115*, 7589. (e) Rus, D.; Tolley, M. T. *Nature* **2015**, *521*, 467. (f) Slater, A. G.; Cooper, A. I. *Science* **2015**, *348*, 6238.

(2) (a) Liu, Y.; Tang, Y.; Barashkov, N. N.; Irgibaeva, I. S.; Lam, J. W. Y.; Hu, R. R.; Birimzhanova, D.; Yu, Y.; Tang, B. Z. *J. Am. Chem. Soc.* **2010**, *132*, 13951. (b) Kim, K.; Tsay, O. G.; Atwood, D. A.; Churchill, D. G. *Chem. Rev.* **2011**, *111*, 5345. (c) Niu, L.-Y.; Guan, Y.-S.; Chen, Y.-Z.; Wu, L.-Z.; Tung, C.-H.; Yang, Q.-Z. *J. Am. Chem. Soc.* **2012**, *134*, 18928. (d) Zhu, H.; Fan, J.; Wang, B.; Peng, X. *Chem. Soc. Rev.* **2015**, *44*, 4337.

(3) (a) Chen, X.; Tian, X.; Shin, I.; Yoon, J. *Chem. Soc. Rev.* **2011**, *40*, 4783. (b) Vendrell, M.; Zhai, D.; Er, J. C.; Chang, Y.-T. *Chem. Rev.* **2012**, *112*, 4391. (c) Yang, S. K.; Shi, X.; Park, S.; Ha, T.; Zimmerman, S. C. *Nat. Chem.* **2013**, *5*, 692. (d) Niu, L.-Y.; Chen, Y.-Z.; Zheng, H.-R.; Wu, L.-Z.; Tung, C.-H.; Yang, Q.-Z. *Chem. Soc. Rev.* **2015**, *44*, 6143.

(4) (a) Leung, C. W. T.; Hong, Y.; Chen, S.; Zhao, E.; Lam, J. W. Y.; Tang, B. Z. *J. Am. Chem. Soc.* **2013**, *135*, 62. (b) Ashton, T. D.; Jolliffe, K. A.; Pfeffer, F. M. *Chem. Soc. Rev.* **2015**, *44*, 4547.

(5) (a) Zhu, M.; Yang, C. *Chem. Soc. Rev.* **2013**, *42*, 4963. (b) Dai, X.; Zhang, Z.; Jin, Y.; Niu, Y.; Cao, H.; Liang, X.; Chen, L.; Wang, J.; Peng, X. *Nature* **2014**, *515*, 96.

(6) (a) Maggini, L.; Bonifazi, D. *Chem. Soc. Rev.* **2012**, *41*, 211. (b) Zhang, Z.; Guo, K.; Li, Y.; Li, X.; Guan, G.; Li, H.; Luo, Y.; Zhao, F.; Zhang, Q.; Wei, B.; Pei, Q.; Peng, H. *Nat. Photonics* **2015**, *9*, 233.

(7) (a) Ajayaghosh, A.; Praveen, V. K.; Vijayakumar, C.; George, S. J. *Angew. Chem., Int. Ed.* **2007**, *46*, 6260. (b) Kuda-Wedagedara, A. N. W.; Wang, C.; Martin, P. D.; Allen, M. J. *J. Am. Chem. Soc.* **2015**, *137*, 4960. (c) Chen, P.; Li, Q.; Grindy, S.; Holten-Andersen, N. *J. Am. Chem. Soc.* **2015**, *137*, 11590.

(8) (a) Birks, J. B. *Photophysics of Aromatic Molecules*; Wiley: London, 1970. (b) Chen, C.-T. *Chem. Mater.* **2004**, *16*, 4389.

(9) (a) Hecht, S.; Fréchet, J. M. J. *Angew. Chem., Int. Ed.* **2001**, *40*, 74. (b) Hoeben, F. J. M.; Jonkheijm, P.; Meijer, E. W.; Schenning, A. P. H.

DOI: 10.1021/jacs.5b10130
J. Am. Chem. Soc. 2015, 137, 15276−15286

J. *Chem. Rev.* **2005**, *105*, 1491. (c) Zhang, X.; Rehm, S.; Safont-Sempere, M. M.; Würthner, F. *Nat. Chem.* **2009**, *1*, 623. (d) Biedermann, F.; Elmalem, E.; Ghosh, I.; Nau, W. M.; Scherman, O. A. *Angew. Chem., Int. Ed.* **2012**, *51*, 7739. (e) Ma, Y.; Marszalek, T.; Yuan, Z.; Stangenberg, R.; Pisula, W.; Chen, L.; Müllen, K. *Chem. - Asian J.* **2015**, *10*, 139.

(10) Luo, J.; Xie, Z.; Lam, J. W. Y.; Cheng, L.; Chen, H.; Qiu, C.; Kwok, H. S.; Zhan, X.; Liu, Y.; Zhu, D.; Tang, B. Z. *Chem. Commun.* **2001**, 1740.

(11) (a) Hong, Y.; Lam, J. W. Y.; Tang, B. Z. *Chem. Commun.* **2009**, 4332. (b) Hong, Y.; Lam, J. W. Y.; Tang, B. Z. *Chem. Soc. Rev.* **2011**, *40*, 5361. (c) Ding, D.; Li, K.; Liu, B.; Tang, B. Z. *Acc. Chem. Res.* **2013**, *46*, 2441. (d) Hu, R.; Leung, N. L. C.; Tang, B. Z. *Chem. Soc. Rev.* **2014**, *43*, 4494. (e) Mei, J.; Hong, Y.; Lam, J. W. Y.; Qin, A.; Tang, Y.; Tang, B. Z. *Adv. Mater.* **2014**, *26*, 5429. (f) Kwok, R. T. K.; Leung, C. W. T.; Lam, J. W. Y.; Tang, B. Z. *Chem. Soc. Rev.* **2015**, *44*, 4228.

(12) (a) Wang, M.; Zhang, G.; Zhang, D.; Zhu, D.; Tang, B. Z. *J. Mater. Chem.* **2010**, *20*, 1858. (b) Zhao, Z.; Lam, J. W. Y.; Tang, B. Z. *J. Mater. Chem.* **2012**, *22*, 23726.

(13) Stang, P. J. *J. Am. Chem. Soc.* **2012**, *134*, 11829.

(14) (a) Cotton, F. A.; Lin, C.; Murillo, C. A. *Acc. Chem. Res.* **2001**, *34*, 759. (b) Cotton, F. A.; Lin, C.; Murillo, C. A. *Proc. Natl. Acad. Sci. U. S. A.* **2002**, *99*, 4810.

(15) Stang, P. J.; Olenyuk, B. *Acc. Chem. Res.* **1997**, *30*, 502. (b) Leininger, S.; Olenyuk, B.; Stang, P. J. *Chem. Rev.* **2000**, *100*, 853. (c) Northrop, B. H.; Zheng, Y.-R.; Chi, K.-W.; Stang, P. J. *Acc. Chem. Res.* **2009**, *42*, 1554. (d) Chakrabarty, R.; Mukherjee, P. S.; Stang, P. J. *Chem. Rev.* **2011**, *111*, 6810. (e) Cook, T. R.; Zheng, Y.-R.; Stang, P. J. *Chem. Rev.* **2013**, *113*, 734. (f) Cook, T. R.; Stang, P. J. *Chem. Rev.* **2015**, *115*, 7001.

(16) (a) Pluth, M. D.; Bergman, R. G.; Raymond, K. N. *Acc. Chem. Res.* **2009**, *42*, 1650. (b) Brown, C. J.; Miller, G. M.; Johnson, M. W.; Bergman, R. G.; Raymond, K. N. *J. Am. Chem. Soc.* **2011**, *133*, 11964. (c) Brown, C. J.; Toste, F. D.; Bergman, R. G.; Raymond, K. N. *Chem. Rev.* **2015**, *115*, 3012.

(17) (a) Gianneschi, N. C.; Masar, M. S., III; Mirkin, C. A. *Acc. Chem. Res.* **2005**, *38*, 825. (b) Oliveri, C. G.; Ulmann, P. A.; Wiester, M. J.; Mirkin, C. A. *Acc. Chem. Res.* **2008**, *41*, 1618. (c) Lifschitz, A. M.; Rosen, M. S.; McGuirk, C. M.; Mirkin, C. A. *J. Am. Chem. Soc.* **2015**, *137*, 7252.

(18) (a) Fujita, M.; Tominaga, M.; Hori, A.; Therrien, B. *Acc. Chem. Res.* **2005**, *38*, 369−378. (b) Sun, Q.-F.; Iwasa, J.; Ogawa, D.; Ishido, Y.; Sato, S.; Ozeki, T.; Sei, Y.; Yamaguchi, K.; Fujita, M. *Science* **2010**, *328*, 1144. (c) Harris, K.; Fujita, D.; Fujita, M. *Chem. Commun.* **2013**, *49*, 6703.

(19) (a) Newkome, G. R.; Wang, P.; Moorefield, C. N.; Cho, T. J.; Mohapatra, P. P.; Li, S.; Hwang, S.-H.; Lukoyanova, O.; Echegoyen, L.; Palagallo, J. A.; Iancu, V.; Hla, S.-W. *Science* **2006**, *312*, 1782. (b) Newkome, G. R.; Moorefield, C. N. *Chem. Soc. Rev.* **2015**, *44*, 3954. (c) Xie, T.-Z.; Guo, K.; Guo, Z.; Gao, W.-Y.; Wojtas, L.; Ning, G.-H.; Huang, M.; Lu, X.; Li, J.-Y.; Liao, S.-Y.; Chen, Y.-S.; Moorefield, C. N.; Saunders, M. J.; Cheng, S. Z. D.; Wesdemiotis, C.; Newkome, G. R. *Angew. Chem., Int. Ed.* **2015**, *54*, 9224.

(20) (a) Lee, J.; Farha, O. K.; Roberts, J.; Scheidt, K. A.; Nguyen, S. T.; Hupp, J. T. *Chem. Soc. Rev.* **2009**, *38*, 1450. (b) Farha, O. K.; Hupp, J. T. *Acc. Chem. Res.* **2010**, *43*, 1166. (c) Kreno, L. E.; Leong, K.; Farha, O. K.; Allendorf, M.; Van Duyne, R. P.; Hupp, J. T. *Chem. Rev.* **2012**, *112*, 1105.

(21) (a) De, S.; Mahata, K.; Schmittel, M. *Chem. Soc. Rev.* **2010**, *39*, 1555. (b) Saha, M. L.; Schmittel, M. *J. Am. Chem. Soc.* **2013**, *135*, 17743. (c) Saha, M. L.; Neogi, S.; Schmittel, M. *Dalton Trans.* **2014**, *43*, 3815.

(22) (a) Nakamura, T.; Ube, H.; Shionoya, M. *Angew. Chem., Int. Ed.* **2013**, *52*, 12096. (b) Nakamura, T.; Ube, H.; Miyake, R.; Shionoya, M. *J. Am. Chem. Soc.* **2013**, *135*, 18790. (c) Kubota, R.; Tashiro, S.; Shiro, M.; Shionoya, M. *Nat. Chem.* **2014**, *6*, 913.

(23) (a) Mal, P.; Breiner, B.; Rissanen, K.; Nitschke, J. R. *Science* **2009**, *324*, 1697. (b) Smulders, M. M.; Riddell, I. A.; Browne, C.; Nitschke, J. R. *Chem. Soc. Rev.* **2013**, *42*, 1728. (c) Castilla, A. M.; Ramsay, W. J.; Nitschke, J. R. *Acc. Chem. Res.* **2014**, *47*, 2063. (d) Wood, C. S.; Ronson, T. K.; Belenguer, A. M.; Holstein, J. J.; Nitschke, J. R. *Nat. Chem.* **2015**, *7*, 354.

(24) (a) Han, Y.-F.; Jin, G.-X. *Acc. Chem. Res.* **2014**, *47*, 3571. (b) Huang, S.-L.; Lin, Y.-J.; Li, Z.-H.; Jin, G.-X. *Angew. Chem., Int. Ed.* **2014**, *53*, 11218. (c) Zhang, Y.-Y.; Shen, X.-Y.; Weng, L.-H.; Jin, G.-X. *J. Am. Chem. Soc.* **2014**, *136*, 15521.

(25) (a) Kishi, N.; Li, Z.; Yoza, K.; Akita, M.; Yoshizawa, M. *J. Am. Chem. Soc.* **2011**, *133*, 11438. (b) Bivaud, S.; Balandier, J. Y.; Chas, M.; Allain, M.; Goeb, S.; Sallé, M. *J. Am. Chem. Soc.* **2012**, *134*, 11968. (c) Mahata, K.; Frischmann, P. D.; Würthner, F. *J. Am. Chem. Soc.* **2013**, *135*, 15656. (d) Li, K.; Zhang, L.-Y.; Yan, C.; Wei, S.-C.; Pan, M.; Zhang, L.; Su, C.-Y. *J. Am. Chem. Soc.* **2014**, *136*, 4456. (e) Han, M.; Engelhard, D. M.; Clever, G. H. *Chem. Soc. Rev.* **2014**, *43*, 1848. (f) Yoshizawa, M.; Klosterman, T. K. *Chem. Soc. Rev.* **2014**, *43*, 1885. (g) Chen, L.-J.; Zhao, G.-Z.; Jiang, B.; Sun, B.; Wang, M.; Xu, L.; He, J.; Abliz, Z.; Tan, H.; Li, X.; Yang, H.-B. *J. Am. Chem. Soc.* **2014**, *136*, 5993. (h) Wang, M.; Wang, C.; Hao, X.-Q.; Liu, J.; Li, X.; Xu, C.; Lopez, A.; Sun, L.; Song, M.-P.; Yang, H.-B.; Li, X. *J. Am. Chem. Soc.* **2014**, *136*, 6664. (i) Wang, M.; Wang, C.; Hao, X.-Q.; Li, X.; Vaughn, T. J.; Zhang, Y.-Y.; Yu, Y.; Li, Z.-Y.; Song, M.-P.; Yang, H.-B.; Li, X. *J. Am. Chem. Soc.* **2014**, *136*, 10499. (j) Samanta, D.; Mukherjee, P. S. *J. Am. Chem. Soc.* **2014**, *136*, 17006. (k) Löffler, S.; Lübben, J.; Krause, L.; Stalke, D.; Dittrich, B.; Clever, G. H. *J. Am. Chem. Soc.* **2015**, *137*, 1060. (l) Sun, B.; Wang, M.; Lou, Z.; Huang, M.; Xu, C.; Li, X.; Chen, L.-J.; Yu, Y.; Davis, G. L.; Xu, B.; Yang, H.-B.; Li, X.-P. *J. Am. Chem. Soc.* **2015**, *137*, 1556. (m) Yan, L.-L.; Tan, C.-H.; Zhang, G.-L.; Zhou, L.-P.; Bünzli, J.-C.; Sun, Q.-F. *J. Am. Chem. Soc.* **2015**, *137*, 8550. (n) Zhang, G.-L.; Zhou, L.-P.; Yuan, D.-Q.; Sun, Q.-F. *Angew. Chem., Int. Ed.* **2015**, *54*, 9844. (o) Bhat, I. A.; Samanta, D.; Mukherjee, P. S. *J. Am. Chem. Soc.* **2015**, *137*, 9497.

(26) (a) Gramage-Doria, F.; Hessels, J.; Leenders, S. H. A. M.; Tröppner, O.; Dürr, M.; Ivanović-Burmazović, I.; Reek, J. N. H. *Angew. Chem., Int. Ed.* **2014**, *53*, 13380. (b) García-Simón, C.; Gramage-Doria, F.; Raoufmoghaddam, S.; Parella, T.; Costas, M.; Ribas, X.; Reek, J. N. H. *J. Am. Chem. Soc.* **2015**, *137*, 2680.

(27) (a) Yoshizawa, M.; Tamura, M.; Fujita, M. *Science* **2006**, *312*, 251. (b) Inokuma, Y.; Kawano, M.; Fujita, M. *Nat. Chem.* **2011**, *3*, 349.

(28) (a) Yang, H.-B.; Ghosh, K.; Northrop, B. H.; Zheng, Y.-R.; Lyndon, M. M.; Muddiman, D. C.; Stang, P. J. *J. Am. Chem. Soc.* **2007**, *129*, 14187. (b) Yamashina, M.; Sartin, M. M.; Sei, Y.; Akita, M.; Takeuchi, S.; Tahara, T.; Yoshizawa, M. *J. Am. Chem. Soc.* **2015**, *137*, 9266. (c) Roy, B.; Ghosh, A. K.; Srivastava, S.; D'Silva, P.; Mukherjee, P. S. *J. Am. Chem. Soc.* **2015**, *137*, 11916.

(29) (a) Li, S.; Huang, J.; Cook, T. R.; Pollock, J. B.; Kim, H.; Chi, K.-W.; Stang, P. J. *J. Am. Chem. Soc.* **2013**, *135*, 2084. (b) Li, S.; Huang, J.; Zhou, F.; Cook, T. R.; Yan, X.; Ye, Y.; Zhu, B.; Zheng, B.; Stang, P. J. *J. Am. Chem. Soc.* **2014**, *136*, 5908. (c) Lee, H.; Elumalai, P.; Singh, N.; Kim, H.; Lee, S. U.; Chi, K.-W. *J. Am. Chem. Soc.* **2015**, *137*, 4674. (d) Zhu, R.; Lübben, J.; Dittrich, B.; Clever, G. H. *Angew. Chem., Int. Ed.* **2015**, *54*, 2796.

(30) (a) Murase, T.; Sato, S.; Fujita, M. *Angew. Chem., Int. Ed.* **2007**, *46*, 1083. (b) Takao, K.; Suzuki, K.; Ichijo, T.; Sato, S.; Asakura, H.; Teramura, K.; Kato, K.; Ohba, T.; Morita, T.; Fujita, M. *Angew. Chem., Int. Ed.* **2012**, *51*, 5893.

(31) (a) Yan, X.; Li, S.; Cook, T. R.; Ji, X.; Yao, Y.; Pollock, J. B.; Shi, Y.; Yu, G.; Li, J.; Huang, F.; Stang, P. J. *J. Am. Chem. Soc.* **2013**, *135*, 14036. (b) Wei, P.; Cook, T. R.; Yan, X.; Huang, F.; Stang, P. J. *J. Am. Chem. Soc.* **2014**, *136*, 15497.

(32) (a) Yan, X.; Li, S.; Pollock, J. B.; Cook, T. R.; Chen, J.; Zhang, Y.; Ji, X.; Yu, Y.; Huang, F.; Stang, P. J. *Proc. Natl. Acad. Sci. U. S. A.* **2013**, *110*, 15585. (b) Yan, X.; Jiang, B.; Cook, T. R.; Zhang, Y.; Li, J.; Yu, Y.; Huang, F.; Yang, H.-B.; Stang, P. J. *J. Am. Chem. Soc.* **2013**, *135*, 16813. (c) Li, Z.-Y.; Zhang, Y.; Zhang, C.-W.; Chen, L.-J.; Wang, C.; Tan, H.; Yu, Y.; Li, X.; Yang, H.-B. *J. Am. Chem. Soc.* **2014**, *136*, 8577. (d) Yan, X.; Cook, T. R.; Pollock, J. B.; Wei, P.; Zhang, Y.; Yu, Y.; Huang, F.; Stang, P. J. *J. Am. Chem. Soc.* **2014**, *136*, 4460. (e) Yan, X.; Xu, J.-F.; Cook, T. R.; Huang, F.; Yang, Q.-Z.; Tung, C.-H.; Stang, P. J.

DOI: 10.1021/jacs.5b10130
J. Am. Chem. Soc. 2015, 137, 15276−15286

Proc. Natl. Acad. Sci. U. S. A. **2014**, *111*, 8717. (f) Foster, J. A.; Parker, R. M.; Belenguer, A. M.; Kishi, N.; Sutton, S.; Abell, C.; Nitschke, J. R. *J. Am. Chem. Soc.* **2015**, *137*, 9722.

(33) (a) Jung, H.; Dubey, A.; Koo, H. J.; Vajpayee, V.; Cook, T. R.; Kim, H.; Kang, S. C.; Stang, P. J.; Chi, K.-W. *Chem. - Eur. J.* **2013**, *19*, 6709. (b) Cook, T. R.; Vajpayee, V.; Lee, M. H.; Stang, P. J.; Chi, K.-W. *Acc. Chem. Res.* **2013**, *46*, 2464. (c) Zheng, Y.-R.; Suntharalingam, K.; Johnstone, T. C.; Lippard, S. J. *Chem. Sci.* **2015**, *6*, 1189.

(34) (a) Po, C.; Tam, A. Y.-Y.; Wong, K. M.-C.; Yam, V. W.-W. *J. Am. Chem. Soc.* **2011**, *133*, 12136. (b) Kent, C. A.; Liu, D.; Meyer, T. J.; Lin, W. *J. Am. Chem. Soc.* **2012**, *134*, 3991. (c) Pollock, J. B.; Schneider, G. L.; Cook, T. R.; Davies, A. S.; Stang, P. J. *J. Am. Chem. Soc.* **2013**, *135*, 13676.

(35) (a) Shustova, N. B.; McCarthy, B. D.; Dincă, M. *J. Am. Chem. Soc.* **2011**, *133*, 20126. (b) Shustova, N. B.; Ong, T.-C.; Cozzolino, A. F.; Michaelis, V. K.; Griffin, R. G.; Dincă, M. *J. Am. Chem. Soc.* **2012**, *134*, 15061. (c) Wei, Z.; Gu, Z.-Y.; Arvapally, R. K.; Chen, Y.-P.; McDougald, R. N., Jr.; Ivy, J. F.; Yakovenko, A. A.; Feng, D.; Omary, M. A.; Zhou, H.-C. *J. Am. Chem. Soc.* **2014**, *136*, 8269. (d) Zhang, M.; Feng, G.; Song, Z.; Zhou, Y.-P.; Chao, H.-Y.; Yuan, D.; Tan, T. T. Y.; Guo, Z.; Hu, Z.; Tang, B. Z.; Liu, B.; Zhao, D. *J. Am. Chem. Soc.* **2014**, *136*, 7241. (e) Zhang, Q.; Su, J.; Feng, D.; Wei, Z.; Zou, X.; Zhou, H.-C. *J. Am. Chem. Soc.* **2015**, *137*, 10064.

(36) (a) Liang, G.; Lam, J. W. Y.; Qin, W.; Li, J.; Xie, N.; Tang, B. Z. *Chem. Commun.* **2014**, *50*, 1725. (b) Wang, P.; Yan, X.; Huang, F. *Chem. Commun.* **2014**, *50*, 5017. (c) Song, N.; Chen, D.-X.; Qiu, Y.-C.; Yang, X.-Y.; Xu, B.; Tian, W.; Yang, Y.-W. *Chem. Commun.* **2014**, *50*, 8231. (d) Wu, J.; Sun, S.; Feng, X.; Shi, J.; Hu, X.-Y.; Wang, L. *Chem. Commun.* **2014**, *50*, 9122. (e) Bai, W.; Wang, Z.; Tong, J.; Mei, J.; Qin, A.; Sun, J. Z.; Tang, B. Z. *Chem. Commun.* **2015**, *51*, 1089. (f) He, L.; Liu, X.; Liang, J.; Cong, Y.; Weng, Z.; Bu, W. *Chem. Commun.* **2015**, *51*, 7148.

(37) Zhao, J.; Yang, D.; Zhao, Y.; Yang, X.-J.; Wang, Y.-Y.; Wu, B. *Angew. Chem., Int. Ed.* **2014**, *53*, 6632.

(38) (a) Sun, F.; Zhang, G.; Zhang, D.; Xue, L.; Jiang, H. *Org. Lett.* **2011**, *13*, 6378. (b) Gui, S.; Huang, Y.; Hu, F.; Jin, Y.; Zhang, G.; Yan, L.; Zhang, D.; Zhao, R. *Anal. Chem.* **2015**, *87*, 1470.

(39) (a) Peng, H.-Q.; Xu, J.-F.; Chen, Y.-Z.; Wu, L.-Z.; Tung, C.-H.; Yang, Q.-Z. *Chem. Commun.* **2014**, *50*, 1334. (b) Zhang, C.; Li, Y.; Xue, X.; Chu, P.; Liu, C.; Yang, K.; Jiang, Y.; Chen, W.-Q.; Zou, G.; Liang, X.-J. *Chem. Commun.* **2015**, *51*, 4168. (c) Suresh, V. M.; De, A.; Maji, T. K. *Chem. Commun.* **2015**, *51*, 14678.

(40) Yu, G.; Tang, G.; Huang, F. *J. Mater. Chem. C* **2014**, *2*, 6609.

(41) (a) Xu, L.; Jiang, L.; Drechsler, M.; Sun, Y.; Liu, Z.; Huang, J.; Tang, B. Z.; Li, Z.; Stuart, M. A. C.; Yan, Y. *J. Am. Chem. Soc.* **2014**, *136*, 1942. (b) Liu, X.; Zeng, Y.; Liu, J.; Li, P.; Zhang, D.; Zhang, X.; Yu, T.; Chen, J.; Yang, G.; Li, Y. *Langmuir* **2015**, *31*, 4386. (c) Chen, L.-J.; Ren, Y.-Y.; Wu, N.-W.; Sun, B.; Ma, J.-Q.; Zhang, L.; Tan, H.; Liu, M.; Li, X.; Yang, H.-B. *J. Am. Chem. Soc.* **2015**, *137*, 11725.

(42) (a) Yuan, W. Z.; Lu, P.; Chen, S.; Lam, J. W. Y.; Wang, Z.; Liu, Y.; Kwok, H. S.; Ma, Y.; Tang, B. Z. *Adv. Mater.* **2010**, *22*, 2159. (b) Chang, Z.-F.; Jing, L.-M.; Wei, C.; Dong, Y.-P.; Ye, Y.-C.; Zhao, Y. S.; Wang, J.-L. *Chem. - Eur. J.* **2015**, *21*, 8504.

(43) (a) Lehn, J.-M. *Angew. Chem., Int. Ed.* **2013**, *52*, 2836. (b) Mattia, E.; Otto, S. *Nat. Nanotechnol.* **2015**, *10*, 111.

(44) Yan, X.; Cook, T. R.; Wang, P.; Huang, F.; Stang, P. J. *Nat. Chem.* **2015**, *7*, 342.

(45) Frisch, M. J.; Trucks, G. W.; Schlegel, H. B.; Scuseria, G. E.; Robb, M. A.; Cheeseman, J. R.; Scalmani, G.; Barone, V.; Mennucci, B.; Petersson, G. A.; Nakatsuji, H.; Caricato, M.; Li, X.; Hratchian, H. P.; Izmaylov, A. F.; Bloino, J.; Zheng, G.; Sonnenberg, J. L.; Hada, M.; Ehara, M.; Toyota, K.; Fukuda, R.; Hasegawa, J.; Ishida, M.; Nakajima, T.; Honda, Y.; Kitao, O.; Nakai, H.; Vreven, T.; Montgomery, J. A., Jr.; Peralta, J. E.; Ogliaro, F.; Bearpark, M.; Heyd, J. J.; Brothers, E.; Kudin, K. N.; Staroverov, V. N.; Kobayashi, R.; Normand, J.; Raghavachari, K.; Rendell, A.; Burant, J. C.; Iyengar, S. S.; Tomasi, J.; Cossi, M.; Rega, N.; Millam, J. M.; Klene, M.; Knox, J. E.; Cross, J. B.; Bakken, V.; Adamo, C.; Jaramillo, J.; Gomperts, R.; Stratmann, R. E.; Yazyev, O.; Austin, A. J.; Cammi, R.; Pomelli, C.; Ochterski, J. W.; Martin, R. L.; Morokuma, K.; Zakrzewski, V. G.; Voth, G. A.; Salvador, P.; Dannenberg, J. J.; Dapprich, S.; Daniels, A. D.; Farkas, O.; Foresman, J. B.; Ortiz, J. V.; Cioslowski, J.; Fox, D. J. *Gaussian09*, Revision C.01; Gaussian, Inc.: Wallingford, CT, 2010.

(46) (a) Becke, A. D. *J. Chem. Phys.* **1993**, *98*, 5648. (b) Lee, C.; Yang, W.; Parr, R. G. *Phys. Rev. B: Condens. Matter Mater. Phys.* **1988**, *37*, 785.

(47) Hehre, W. J.; Ditchfield, R.; Pople, J. A. *J. Chem. Phys.* **1972**, *56*, 2257.

(48) Hay, P. J.; Wadt, W. R. *J. Chem. Phys.* **1985**, *82*, 299.

(49) Parrott, E. P. J.; Tan, N. Y.; Hu, R. R.; Zeitler, J. A.; Tang, B. Z.; Pickwell-MacPherson, E. *Mater. Horiz.* **2014**, *1*, 251.

(50) (a) Kartha, K. K.; Babu, S. S.; Srinivasan, S.; Ajayaghosh, A. *J. Am. Chem. Soc.* **2012**, *134*, 4834. (b) Nagarkar, S. S.; Joarder, B.; Chaudhari, A. K.; Mukherjee, S.; Ghosh, S. K. *Angew. Chem., Int. Ed.* **2013**, *52*, 2881. (c) Shanmugaraju, S.; Bar, A. K.; Jadhav, H.; Moon, D.; Mukherjee, P. S. *Dalton Trans.* **2013**, *42*, 2998. (d) Shanmugaraju, S.; Mukherjee, P. S. *Chem. - Eur. J.* **2015**, *21*, 6656. (e) Sun, X.; Wang, Y.; Lei, Y. *Chem. Soc. Rev.* **2015**, *44*, 8019.

(51) Qin, A.; Lam, J. W. Y.; Tang, L.; Jim, C. K. W.; Zhao, H.; Sun, J.; Tang, B. Z. *Macromolecules* **2009**, *42*, 1421.

(52) Liu, J.; Zhong, Y.; Lu, P.; Hong, Y.; Lam, J. W. Y.; Faisal, M.; Yu, Y.; Wong, K. S.; Tang, B. Z. *Polym. Chem.* **2010**, *1*, 426.

(53) (a) Shanmugaraju, S.; Joshi, S. A.; Mukherjee, P. S. *Inorg. Chem.* **2011**, *50*, 11736. (b) Samanta, D.; Mukherjee, P. S. *Dalton Trans.* **2013**, *42*, 16784. (c) Bhowmick, S.; Chakraborty, S.; Das, A.; Nallapeta, S.; Das, N. *Inorg. Chem.* **2015**, *54*, 8994.

DOI: 10.1021/jacs.5b10130
J. Am. Chem. Soc. 2015, 137, 15276−15286